Nanometre scale surface modification in a needle–plate exploding system

2005 J. Phys.: Condens. Matter 17 5327

(http://iopscience.iop.org/0953-8984/17/35/001)

INSTITUTE OF PHYSICS PUBLISHING JOURNAL OF PHYSICS: CONDENSED MATTER

J. Phys.: Condens. Matter **17** (2005) 5327–5334 doi:10.1088/0953-8984/17/35/001

Nanometre scale surface modification in a needle–plate exploding system

Vandana and P Sen[1]

School of Physical Sciences, Jawaharlal Nehru University, New Delhi-110067, India

E-mail: prasenjitsen@vsnl.net

Received 15 May 2005, in final form 26 June 2005
Published 19 August 2005
Online at stacks.iop.org/JPhysCM/17/5327

Abstract

Exploding a wire on a metallic plate, we demonstrate reorganization of the metallic surface at different length scales. While optical microscopy shows clear concentric ring patterns, atomic force microscopy provide details of nanometre sized entities that constitute these rings. The size of these entities scales with the wire dimensions and applied explosion voltages. From fluctuations in the plasma current recorded during the process, the particle formation is seen to be a self-organization process.

(Some figures in this article are in colour only in the electronic version)

1. Introduction

Controlled surface modification of metals is an area of interest both for fundamental as well as applied science. While microstructures are important for the strength of a material, reorganized surface atoms are desired with length scales considerably smaller than 1 μm to the order of a few nanometres, for designing tuned electronic properties. A method of doing this is to induce pattern formations in metals, whose instances are rare. Situations where patterns are observed include ion irradiation and sputtered surfaces [1], dendritic growth [2] and electrochemical dissolution of metals [3]. All these examples are typical of problems in pattern formation that take place far from equilibrium.

Nonlinearities introduced in a dynamical system are known to induce spatial patterns that are sometimes stationary, travelling or disordered in space and time. We employ electro-explosion of wires to introduce nonlinearities in a metal. Explosion of wires [4] is achieved when a very high current, suddenly applied to a thin conducting wire, causes it to fragment explosively. Various experimental and theoretical investigations of this phenomenon exist [5–14]. A study of the literature shows that wire explosion and fragmentation generally tend to proceed in the following manner [13, 14]: (a) heating of wire and wire melting;

[1] Author to whom any correspondence should be addressed.

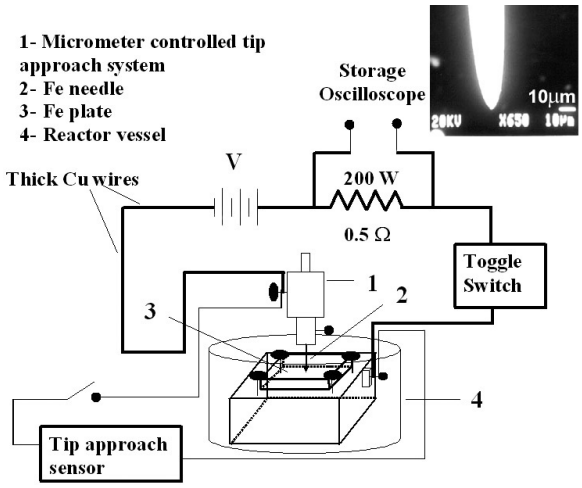

Figure 1. Schematic diagram showing the arrangement employed to perform a needle–plate explosion. The current through the set-up is recorded across a 200 W resistor and stored in an oscilloscope. During the experiment, the reactor vessel is filled with water. A micrometer is driven in steps and a current feedback controls the tip–plate approach. An inset shows SEM of a typical metallic tip with diameter 1 μm, prior to explosion.

(b) wire explosion (evaporation) and formation of a high density core surrounded by low density ionized corona; (c) coronal compression by self-induced magnetic fields; and (d) fast expansion of explosion products resulting in shock wave generation.

In this paper, we present results from exploding a metallic needle on a metal plate. We establish this to be similar to the phenomenon of exploding single wires, by monitoring the time evolution of the current through the wire. The metallic surface reorganizes as a result of the shock waves generated, into nanometre sized entities whose scaling behaviour is reported. We further show that fluctuations in the recorded plasma current are not random events but correlated and thus reflect self-organization behaviour.

2. Sample preparation and characterization

Single-wire single-explosion (SWSE) experiments were carried out using iron tips and polished iron plates (all plates measure 10 mm $\times$ 10 mm $\times$ 0.5 mm) in the voltage range 12–48 V DC. The experimental arrangement consists of an iron plate as one of the electrodes and the wire as the other electrode (figure 1). Thick copper or silver coated copper wires measuring 241 cm in overall length and 1.5 mm in diameter were employed to carry the current to the needle–plate arrangement. A 0.5 Ω, 200 W resistor in series was employed to measure the current through the wires, recorded employing a digital oscilloscope (model Tektronix TDS 1002) with a base time resolution of 5 ns. The explosions were carried out in a specially designed reactor vessel under water. X-ray diffraction patterns and EDAX measurements confirmed the purity of the wires and plates. The iron tips were prepared by electrochemical etching of 0.37 mm diameter iron wire in a $FeSO_4$ solution (pH controlled). Tip diameters were measured by a scanning electron microscope (SEM) and an optical microscope. The iron plates were polished to a roughness of 50–500 nm, confirmed by atomic force microscope (AFM) measurements. The AFM measurements reported here were carried out employing the CP-Research model from ThermoMicroscopes, USA.

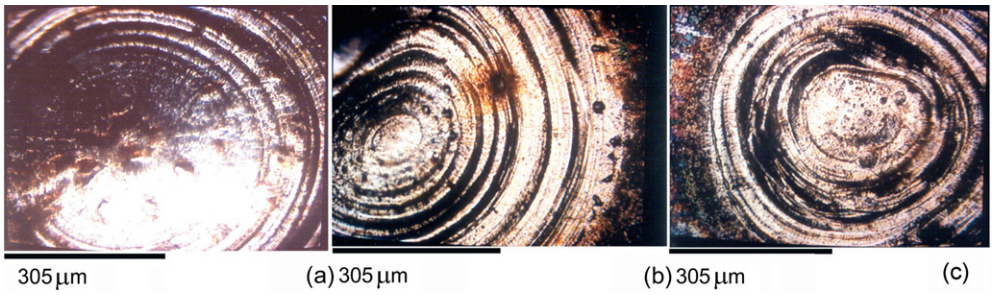

Figure 2. Optical micrographs showing results from explosions in the needle–plate configuration for Fe/Fe systems (plate-positive; see the text). (a) Fe/Fe_{370} system, voltage = 48 V; (b) Fe/Fe_{30} system, voltage = 48 V; (c) Fe/Fe_{25} system, voltage = 36 V.

In order to achieve a single spark, a special arrangement is designed to bring the tip close to the stationary plate in a controlled fashion. On achieving first contact, the movement of the tip is stopped. A toggle switch is then activated to connect the arrangement to a battery bank. As the initial spark breaks the circuit with considerable tip destruction on a microscopic scale, multiple sparks are eliminated. Water helps in collection of outward moving exploded wire and plate material, facilitating observation of the modified surface.

3. Results and discussion

3.1. Optical microscopy

In figure 2, we show optical micrographs of SWSE results from exploding iron tips with diameter = 370, 30 and 25 μm on an iron plate (hereafter referred to as Fe/Fe_{370}, Fe/Fe_{30} and Fe/Fe_{25} systems) while holding the plate with a positive polarity (48 V for Fe/Fe_{370} and Fe/Fe_{30} systems and 36 V for the Fe/Fe_{25} system) compared to the needle (plate-positive case). The figure clearly shows rings emanating from the point of contact made by the respective tips with the iron plate. The rings die out at the extreme edge of circles whose diameters for the Fe/Fe systems are 1425 μm (Fe/Fe_{370}), 1091 μm (Fe/Fe_{30}) and 856 μm (Fe/Fe_{25}).

The following observations are common to all the tips exploded: (a) evolution of concentric rings emanating from the point of contact where the wire exploded and (b) the presence of internal structure in all the rings. The lateral extent of the rings on the plate surface, as measured by the diameter of the rings, scales with the tip diameter. This has relevance for the energy deposited into the metal surface, as will be discussed later.

We next try to understand the origin of the rings. As these are incorporated by transformation of an otherwise flat metal surface (of the order of a few nanometres as measured by AFM), melting of the metal is a prerequisite for their formation. The melting is initiated at the point of tip–plate contact, while the high current density through the metal plate melts the metal with circular symmetry as the electrons travel from tip to plate. The spatial extent of the molten disc will then be determined by the power dissipated by the metal plate. Despite the lack of symmetry in our system, we assume a similarity with the exploding wire phenomena, whereby the molten metal (in step (a) as indicated above) is finally subjected to a shock wave (step (d)). The pattern could be a result of a series of shock wavefronts travelling through the molten metal and freezing at the boundary, or due to standing wave formation. To verify this, we measure the width of the bands formed within the ring. In the case of a disturbance starting from the centre and proceeding outwards, the width of a single band would widen due

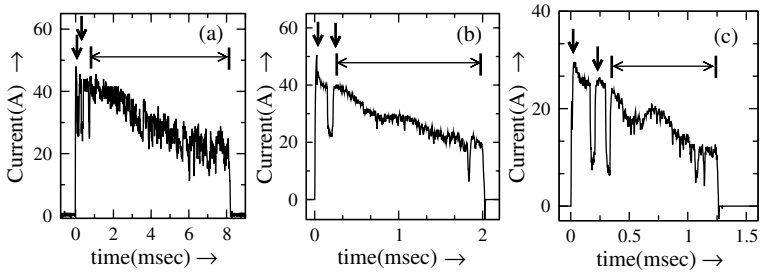

Figure 3. Time evolution of current through the needle–plate configuration during explosion for Fe/Fe systems (plate-positive). (a) Fe/Fe_{370} system, voltage = 48 V; (b) Fe/Fe_{30} system, voltage = 48 V; (c) Fe/Fe_{25} system, voltage = 36 V. Vertical arrows in each plot identify the first and second peaks in the time evolution of the current during explosion (section 3.2). The region marked by a line having double-sided arrows has been employed to study the spectral density (see the text).

to dispersion through the molten metal plate. However, the measured values of selected bands at the explosion centre and periphery (reported here for Fe/Fe with tip diameter = 30 μm) indicate that these are reasonably constant with a value of 4.77 ± 0.01 μm. Hence we propose that these are standing waves formed following the shock wave generation in the molten metal, which can now be visualized as a vibrating liquid surface.

3.2. Time evolution of current during explosion

To understand how well the needle–plate exploding system mimics the traditional wire explosion phenomena [13, 14], we study the time evolution of the process and show, in figure 3, plots of the current flowing through the needle–plate configuration during the explosion event for all the Fe/Fe systems. This plot is a real-time map of the SWSE event and a typical observation is given below. Following closure of the toggle switch, the current increases to show a maximum after which it drops to a low value (first current peak), increasing again, peaking and reducing to a stable value after some time (second current peak). The stable current value is maintained for a long time, after which the current goes to zero. The first current peak represents heating, melting and then explosion, i.e., evaporation of wire following toggle switch activation ($t = 0$), like in reports by other workers [13]. The resulting gas is momentarily at very high density and hence electrons do not acquire sufficient energy to produce ionization by impact. Hence current continues to flow at a constant, low rate restricted by the limited supply of charge carriers, representing a dwell time (or dead time) between the two current peaks [14]. The high gas density is short lived as pressure drops, increasing the mean free path for the electrons, resulting in ionization by impact with attendant avalanching. This gives the second stable current peak, which can be called restrike or reignition [13, 14]. According to published literature, at this point, the formation of a high density vaporized gas core surrounded by low density ionized corona starts. Compression of coronal plasma by the self-induced magnetic field produces shock waves, which propagate through the plasma [8]. The current flows in the circuit as long as the two electrodes are in contact and drops to zero as the contact breaks. We have evidence of plasma formation, as the electro-explosion process is accompanied by emission of visible light.

Comparing figures 3(a), (b) and (c), we can see that the inherent process remains the same as outlined above; however, the entire process is scaled down in time for reduced tip diameters. Thus, for the three systems studied, Fe/Fe_{370}, Fe/Fe_{30} and Fe/Fe_{25}, the total time

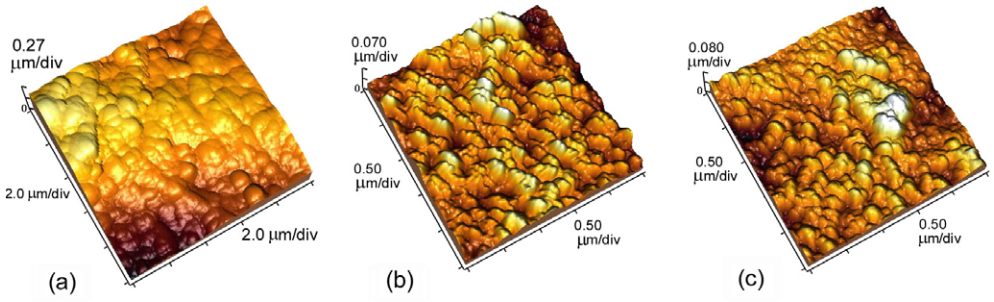

Figure 4. Atomic force microscopy of Fe/Fe systems (plate-positive). (a) Fe/Fe_{370} system, voltage = 48 V; (b) Fe/Fe_{30} system, voltage = 48 V; (c) Fe/Fe_{25} system, voltage = 36 V. These 3D images show the various grain sizes obtained under various exploding conditions.

during which the current passes through the needle–plate system is approximately 8.25, 2 and 1.2 ms respectively. It is expected that a thin wire would carry a smaller value of current (essentially due to the increased resistance of the wire) during the start of the exploding cycle. Comparing figures 3(a) and (c) we can conclude that the energy deposited is likewise reduced, resulting in a total connect time of 8.25 ms for the 370 μm wire at 48 V and 1.2 ms for the 25 μm wire at 36 V. This scaling behaviour in the energy deposition and dissipation allows us to confirm the basic process steps.

3.3. Atomic force microscopy

In figure 4, we show details of each ring with nanometre resolution, employing an AFM working in the non-contact mode. This mode was chosen so as not to have contact with a topologically non-uniform surface. Each ring is seen to consist of smaller particles whose size distribution could provide microscopic details of the processes leading to their formation. Evidence of shock waves producing small (nanosized) particles is indeed there in the literature [12]. It is clear from figure 4 that the particle sizes are largest for Fe/Fe_{370}. As the grains are formed from reorganization in the melt in all the cases studied, it is not clear why they should scale with the tip diameter.

The above results (figures 3 and 4) reveal single-wire electro-explosion-type behaviour in the needle–plate exploding system. The process leading to the formation of the rings can now be further discussed. The exploding needle–plate system brings the plate surface instantaneously to its melting point (typically after 140 μs, as can be seen from close-up pictures of the plots in figure 3). The shock wave generated after the explosion then travels through the melt. In a somewhat similar situation, there is proof of shock wave generation as nonlinear pressure waves, following explosion of single wires in water [12]. In our experiment, the shock waves transform the melt into micron sized particles as our AFM measurements show. Assuming that the shock waves travel with the velocity of sound in Fe (5130 m s^{-1}), it would typically take 500 ns to cover the region modified as a result. This is ∼3 orders of magnitude smaller than the time for which the melt exists (as measured by us; figure 3). From theoretical estimates of the resolidification time available in the literature [15] we likewise conclude that sufficient time exists for the shock waves to travel while the melt survives. The melt however solidifies, starting from the region farthest from the needle–plate contact point, providing a natural boundary that confines the melt. The ring patterns are a result of stationary waves set up in the melt, emanating obviously with cylindrical symmetry from the centre of the figure, which now resembles a vibrating liquid surface.

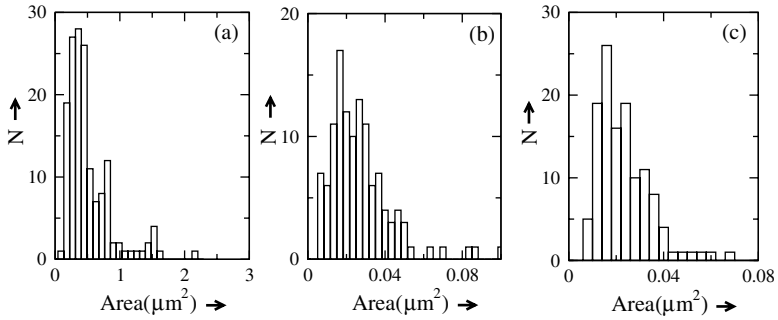

Figure 5. Histogram showing number of grains (N) versus area (μm^2) for Fe/Fe systems (plate-positive) for (a) the Fe/Fe_{370} system; (b) the Fe/Fe_{30} system; (c) the Fe/Fe_{25} system. Grain size variation with diameter and their distribution profile can be seen.

In order to further establish the scaling of the generated particles with tip diameter, we do a grain size analysis of the AFM data. This is presented in figure 5. Errors due to large variation in the background height of the sampled area are avoided by a height threshold (or Z-threshold) selection, which tagged all the grains to be analysed. Individual grains were then selected and their areas determined. The area analysis is presented in figure 5 as a histogram. Area analysis has been chosen as a parameter and not volume analysis, to negate any erroneous estimate in volume from a contribution to the grain height from the system background. The background was not stripped during these estimates. It is clear from figure 5 that explosion of the 370 μm tip (Fe/Fe_{370}) produces the largest grains.

While the influence of the applied electro-explosion voltage does not appear to have any major influence on the grain size (compare figures 5(b) and (c)), the other significant result here is the distribution of grain sizes. The smaller exploding tips have produced a reasonably normal grain size distribution, while the size distribution obtained with the large tip is skewed, with a long exponential tail.

The formation of these particles is a result of the dissipation of energy following the needle–plate explosion, whereby the molten metal surface has recrystallized in this form, allowing the shock waves to reconfigure the molten metal plate. The enhanced surface area (and hence formation of interfaces/defects) of the small metal particles is a result of the energy released by the shock waves, which gets stored in this manner. As this process takes place far away from equilibrium, the configuration gets frozen on a timescale shorter than the time available for the individual particles to coalesce into a single mass again. While sizing down of materials as a result of shock waves is known, it is also established that resolidification of Fe at high pressures and temperatures induces pressure–temperature zones in the liquid with short range nanoscale local structures [16]. As an outcome of this experiment, we indeed collect nanoparticles of Fe in the water medium whose size is less than 15 nm as indicated by disappearance of the ferromagnetic Mössbauer signal [17]. The histogram analysis and the time evolution of the current during the electro-explosion process allow us to understand the scaling behaviour of observed grain sizes with the tip diameter. From figure 3, the current connect time is seen to be largest for the wire with the largest diameter, dissipating the largest amount of heat for the longest time. Hence it can be easily deduced that the melt survives longest. During this time, any small particle produced due to the shock waves would coalesce, leading to larger particle size. This is a possible explanation for scaling of particle size with tip diameter.

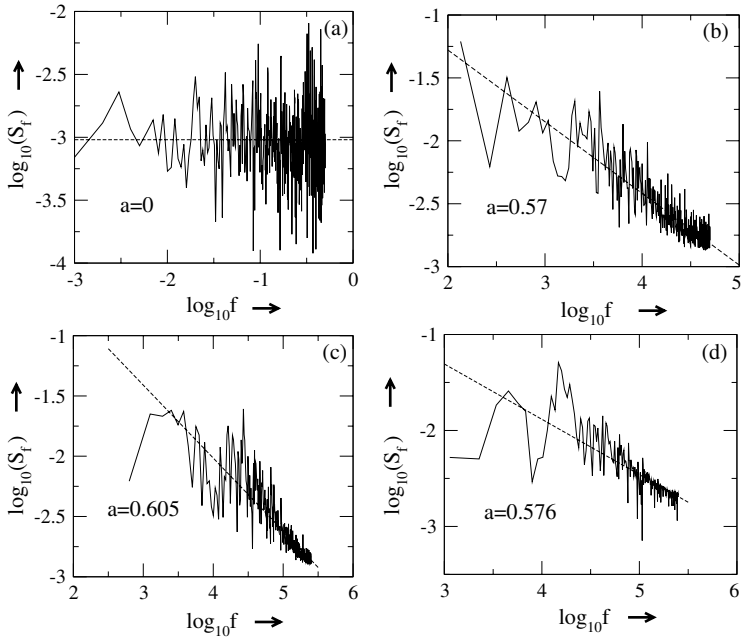

Figure 6. Spectral density dependence is shown by plotting $\log_{10}(S_f)$ versus $\log_{10} f$ (represented by a solid line) for (a) random numbers; (b) the Fe/Fe_{370} system; (c) the Fe/Fe_{30} system; (d) the Fe/Fe_{25} system. The dashed line shows the best fit of the power law $S(f) = \frac{1}{f^a}$ to the solid curve, whose exponent is recorded in the respective figures.

3.4. Plasma current fluctuation study

In order to further analyse the current data, we have identified the fluctuating part of the current in all the current plots of figure 3 with a line having double-sided arrows. This current is a result of plasma formation after restrike or reignition. The ionized plasma carries the current here. This is expected to be a random process during its existence between the tip and the plate. Starting from the current data taken during explosion (as defined by the double-sided arrow), we calculate the spectral density dependence on frequency employing the following steps.

(1) We select a region of current where the shock wave propagates through the plasma.
(2) The natural slope is eliminated by background subtraction using curve fitting. The background is not expected to originate from any physical processes.

The pure fluctuation left after the above procedure is now employed to calculate its autocorrelation plot. In this plot the vertical axis is the autocorrelation coefficient (R_h) and horizontal axis is time lag (h). These are defined as given below.

$R_h = \frac{C_h}{C_0}$, where C_h is the autocovariance function and C_0 is the variance function:

$$C_h = \left(\frac{1}{n}\right)\sum_{l=1}^{n-h}(y_l - y_m)(y_{l+h} - y_m)$$

$$C_0 = \frac{\sum_{l=1}^{n}(y_l - y_m)^2}{n}, \qquad y_m \text{ is the mean value and } h = 1, 2, 3, \ldots, n.$$

Fourier transformation of the autocorrelation plot gives the spectral density. We find the spectral density dependence on frequency by the method of fitting a curve to the spectral plot using the formula

$$S(f) = \frac{1}{f^a},$$

In figures 6(a)–(d), we show $\log_{10} S(f)$ versus $\log_{10} f$ plots starting with a random test data in figure 6(a). The random test data were generated employing a random number generator. As expected, the random data returns a value of $a = 0$ for the exponent of the frequency f. The other values of the exponent are $a = 0.57$ for Fe/Fe_{370}, $a = 0.605$ for Fe/Fe_{30} and 0.576 for Fe/Fe_{25}. Thus the fluctuations in the current data reflect some self-organization process and are not strictly random processes.

4. Conclusions

Our AFM study allows us to show modifications introduced in a metallic surface as a result of electro-explosion. The explosion transforms the region under consideration to consisting of microscopic entities that arrange due to instabilities introduced by the process. The microscopic elements themselves are a result of shock wave propagation and resolidification of the melt. In this regard, although a metal, the system described here belongs to a new universal class wherein the microscopic elements can be large, micron sized objects. Thus the patterns formed can be equated to those in vibrated granular media with intergranular contact forces similar to van der Waals forces.

Acknowledgments

We thank the University Grants Commission, India, for support under the COSIST programme. One of us (Vandana) thanks the Council for Scientific and Industrial Research (CSIR), India, for a fellowship. We also thank Dr R Ghosh, School of Physical Sciences, JNU, for allowing the use of the Tektronix digital storage oscilloscope.

References

[1] Chason E and Aziz M J 2003 *Scr. Mater.* **49** 953
[2] Trivedi R, Liu S and Williams S 2002 *Nat. Mater.* **1** 157
[3] Jaeger N I, Otterstedt R D, Bîrzu A, Green B J and Hudson J L 2002 *Chaos* **12** 231
[4] Graneau P 1983 *Phys. Lett.* A **97** 253
[5] Kalantar D H and Hammer D A 1993 *Phys. Rev. Lett.* **71** 3806
[6] Shelkovenko T A, Pikuz S A, Mingaleev A R and Hammer D A 1999 *Rev. Sci. Instrum.* **70** 667
[7] Gus'kov S Y *et al* 1998 *JETP Lett.* **67** 559
[8] Lee K, Kim D and Kim S 2000 *Phys. Rev. Lett.* **85** 3834
[9] Mosher D, Stephanakis S J, Vitkovitsky I M, Dozier C M, Levine L S and Nagel D J 1973 *Appl. Phys. Lett.* **23** 429
[10] Sarkisov G S, Sasorov P V, Struve K W, McDaniel D H, Gribov A N and Oleinik G M 2002 *Phys. Rev.* E **66** 046413
[11] Sunka P 2001 *Phys. Plasmas* **8** 2587
[12] Lisitsyn I V, Muraki T and Akiyama H 1997 *Appl. Phys. Lett.* **70** 1676
[13] Duselis P U and Kusse B R 2003 *Phys. Plasmas* **10** 565
[14] Chace W G and Moore H K 1959 *Exploding Wires* (New York: Plenum) pp 7–65
[15] Moriarty J A, Belak J F, Rudd R E, Söderlind P, Streitz F H and Yang L H 2002 *J. Phys.: Condens. Matter* **14** 2825
[16] Vezzoli G C 2002 *Mater. Res. Innovat.* **5** 222 and references therein
[17] Sen P, Ghosh J, Alqudami A, Kumar P and Vandana 2003 *Proc. Indian Acad. Sci. Chem. Sci.* **115** 499